# Communications

## Small Broadband Antenna Composed of Dual-Meander Folded Loop and Disk-Loaded Monopole

Wang-Ta Hsieh and Jean-Fu Kiang

***Abstract*—A small broadband antenna composed of a dual-meander folded loop and a disk-loaded monopole is designed and measured. Measurement results confirm a fractional bandwidth of 10.8% with the voltage standing-wave ratio (VSWR) less than 2. The measured radiation efficiency exceeds 65% over the whole band. This antenna has an omnidirectional radiation pattern of vertical polarization in the horizontal plane. The ground plane size is also optimized to achieve the above radiation characteristics.**

***Index Terms*—Broadband, disk-loaded monopole, meander, small antenna.**

### I. Introduction

With the raised demand for wireless devices, small antennas with low profile, light weight and easy fabrication have been widely explored. As the antenna size decreases, its bandwidth tends to reduce because of higher quality factor [1], rendering broadband characteristic a challenging task. Different techniques have been used to reduce the antenna size, including top loading element [2], folded meander-line [3], multi-folded tapered monopole [4], inductive or capacitive loading elements [5], [6]. Space-filling geometry has also been useful to reduce antenna size [7]–[9]. When applying these miniaturization techniques, the antenna efficiency usually degrades and the impedance bandwidth also becomes narrower. Recently, bandwidth enhancement techniques have been studied, including mode coupling between proximity elements [10], [11], adding vertical lines to a meander line [12], dual meander sleeves [13]–[15].

In [16], a 3-D meander dipole antenna with dimensions of $\lambda/11$ is proposed, its fractional impedance bandwidth is about 2.5%. A small spherical wire antenna with diameter of $\lambda/5$ has also been designed, its fractional bandwidth is about 6.7%. In [17], a low-profile metamaterial ring antenna with dimensions of $\lambda/11 \times \lambda/11 \times \lambda/28$ is proposed, its fractional bandwidth is about 6.8% and its measured efficiency is about 54%.

In this work, a small antenna composed of a dual-meander folded loop and a disk-loaded monopole is proposed. A wide impedance bandwidth is achieved by merging the resonant bands of the loop and the monopole with proximity coupling. Design considerations and geometry of the proposed antenna are described in Section II, simulated and measured results are presented and discussed in Sections III and IV, followed by the conclusion.

Manuscript received February 12, 2010; revised September 17, 2010; accepted October 16, 2010. Date of current version May 04, 2011. This work was supported by the National Science Council, Taiwan, ROC under Contract NSC 98-2221-E-002-050.

The authors are with the Department of Electrical Engineering and the Graduate Institute of Communication Engineering, National Taiwan University, Taipei, Taiwan (e-mail: jfkiang@cc.ee.ntu.edu.tw).

Color versions of one or more of the figures in this communication are available online at http://ieeexplore.ieee.org.

Digital Object Identifier 10.1109/TAP.2011.2122236

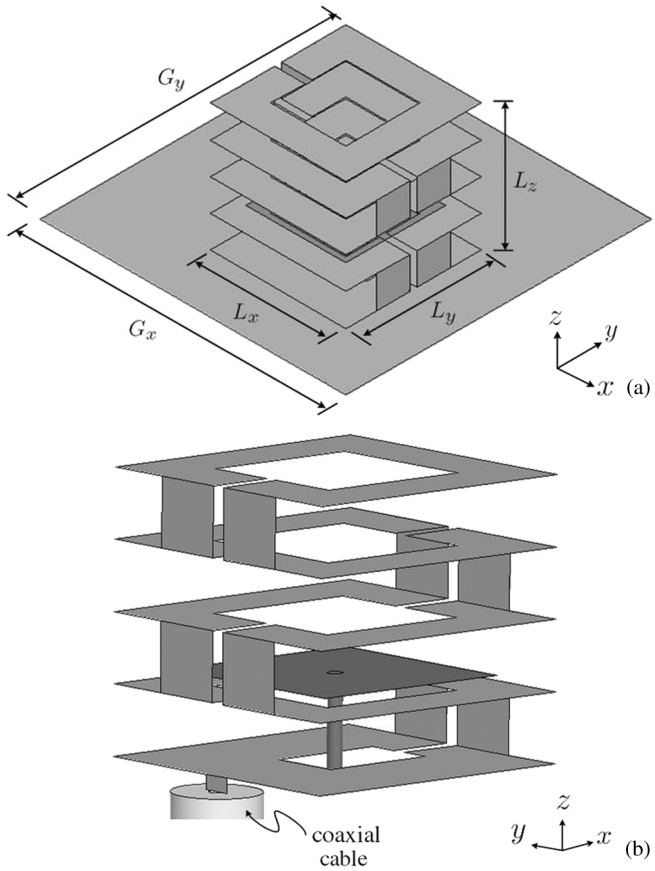


Fig. 1. Panoramic views of the proposed antenna from different looking angles.

### II. Design Considerations

Fig. 1 shows the panoramic views of the dual-meander folded loop antenna and a disk-loaded monopole from two different looking angles. The connection to the 50 Ω coaxial cable and the disk-loaded monopole can be seen in Fig. 1(b). Fig. 2(a) shows the layout of the unfolded dual-meander loop, Fig. 2(b) and 2(c) show the side view and top view, respectively, of the complete design.

The impedance bandwidth of a small antenna is roughly proportional to $1/Q$, where the $Q$ factor of a small antenna with dimension $a$ can be estimated as [1]

$$Q \simeq \frac{1}{(ka)^3}$$

which implies that a smaller antenna is endowed with a larger quality factor. To increase the impedance bandwidth of a dual-meander folded loop, a disk-loaded monopole is placed inside the former. A resonant mode of the disk-loaded monopole is excited by properly adjusting the gap width $g$ between the disk and one surface of the dual meanders.

The resonant bands associated with the dual-meander and the disk-loaded monopole, respectively, merge into one if the width of the square disk, $L_d$, and the gap width $g$ are properly adjusted. Note that larger $L_d$ gives a larger overlapping area between the disk and the dual-meander strips, hence stronger capacitive coupling.

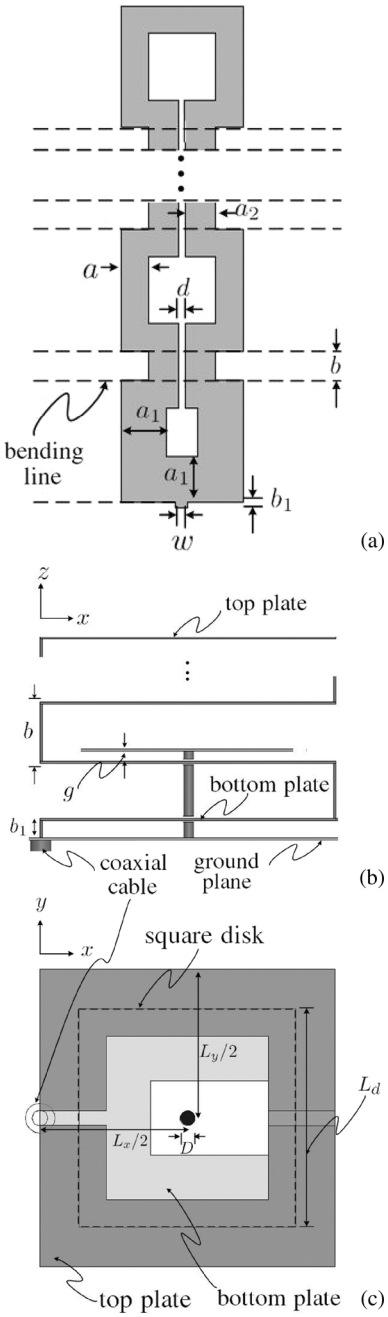


Fig. 2. (a) Layout of unfolded dual meanders with five loops, (b) side view, and (c) top view of proposed antenna.

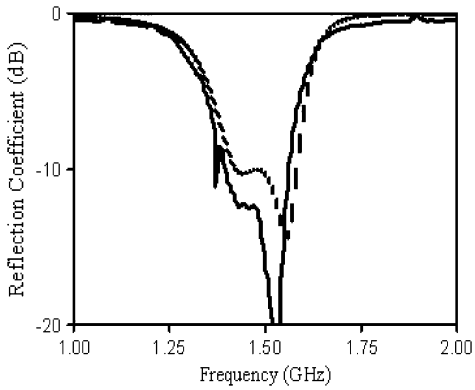


Fig. 3. Measured (——) and simulated (– – –) reflection coefficients, $L_x = 20$, $L_y = 20$, $L_z = 19.8$, $G_x = 130$, $G_y = 110$, $a_1 = 7.5$, $b_1 = 1$, $a_2 = 5$, $a = 4.5$, $b = 4.7$, $d = 1$, $w = 2$, $g = 1$, $D = 1$, $L_d = 14.7$, all in mm.

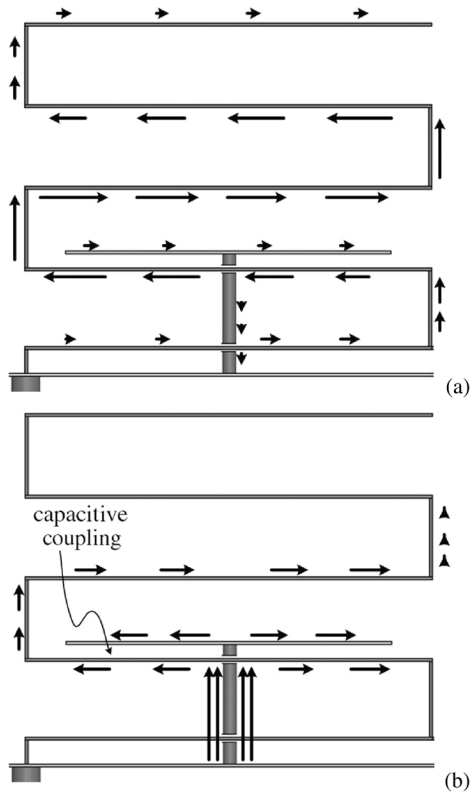


Fig. 4. Simulated surface current distribution at (a) 1.445 GHz and (b) 1.545 GHz.

From another point of view, the disk-loaded monople serves as a parasitic element to the dual-meander loop. Over the band of interest where two resonant bands merge, the electrical length of the dual-meander loop is about one wavelength. The disk-loaded monople is coupled to an adjacent meander strip, effectively extending its electrical length to about one-quarter wavelength. Hence, the physical size of the monopole plus the disk can be much shorter than one-quarter wavelengths.

## III. Results and Discussions

Fig. 3 shows the measured and simulated reflection coefficients of the proposed antenna using HFSS. The antenna takes a cubic space of $20 \times 20 \times 19.8\ \mathrm{mm}^3$, mounted on a $110 \times 130\ \mathrm{mm}^2$ horizontal ground plane. The center frequency is about 1.495 GHz, and the 10-dB bandwidth is about 161 MHz, hence its fractional bandwidth is about 10.8%. The measurement and simulation results match fairly.

Fig. 4(a) and (b) show the side view of the simulated surface current distribution at 1.445 and 1.545 GHz, respectively. The surface current on the meander of the opposite side is the same due to symmetry. The one-wavelength resonance of the dual-meander folded loop appears at about 1.445 GHz. At 1.545 GHz, the quarter-wavelength resonance occurs, the current flows uniformly along the vertical part of the monopole to the disk, then is capacitively coupled to the meander strips underneath, as shown in Fig. 4(b).

Fig. 5 shows the comparison of simulated reflection coefficients with and without the disk-loaded monopole. In the absence of the disk-

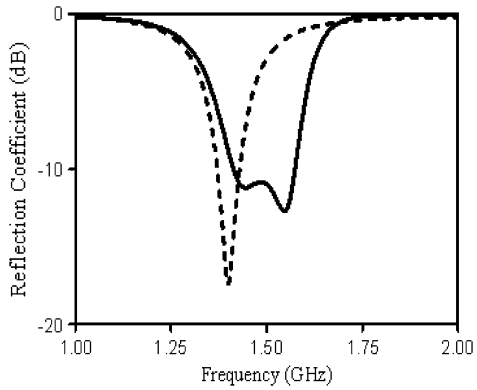


Fig. 5. Comparison of simulated reflection coefficients with (——) and without (– – –) disk-loaded monopole, parameters are the same as in Fig. 3.

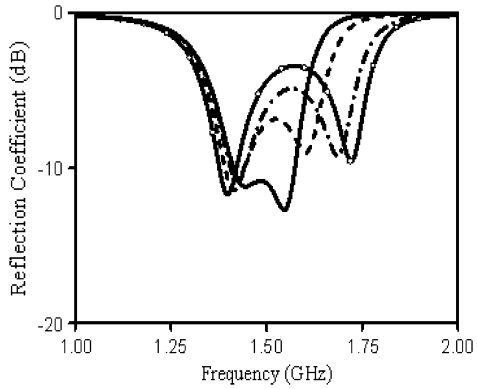


Fig. 6. Simulated reflection coefficients with different disk sizes, ——: $L_d = 14.7$ mm, – – –: $L_d = 14.2$ mm, (— · —): $L_d = 13.7$ mm, — ∘ —: $L_d = 13.2$ mm, other parameters are the same as in Fig. 3.

loaded monopole, the fractional impedance bandwidth of the dual-meander folded loop is about 4.1%. In the presence of the disk-loaded monopole, the impedance bandwidth is increased to 10.8%.

The total length of the dual-meander folded loop is 260 mm, about 0.82 wavelengths at its resonant frequency of 1.4 GHz. The total length of the second resonant path is 43 mm, about 0.22 wavelengths at its resonant frequency of 1.785 GHz, which is measured from the contact point at the ground to the center of the disk, then to the edge of the disk. As shown in Fig. 5, when these two parts are combined, the first resonant frequency increases from 1.4 to 1.445 GHz and the second mode decreases from 1.785 to 1.545 GHz. Such shifts can be explained by the strong capacitive coupling between the disk and the meander strips underneath. Similar concept of tight or strong coupling has also been used to provide broad bandwidth in handset antennas [18].

Fig. 6 shows the simulated reflection coefficients versus the width of the square disk, $L_d$. With a smaller $L_d$, the second mode is shifted to a higher frequency because the capacitive coupling becomes less and the effective length becomes shorter. Intended mode coupling can be achieved by properly adjusting the value of $L_d$.

Fig. 7 shows the simulated reflection coefficients versus the gap width $g$. The resonant frequency of the two modes moves farther apart and the impedance matching become worse with increasing $g$. In this design, we choose $g = 1$ mm.

Fig. 8 shows the measured and simulated radiation pattern at 1.495 GHz, which match reasonably well. The $E_\theta$ pattern in the $x - y$ plane

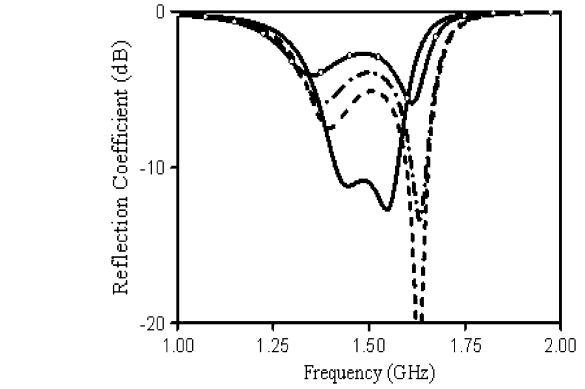


Fig. 7. Simulated reflection coefficients with different gaps between disk and patch, ——: $g = 1$ mm, – – –: $g = 1.5$ mm, — · —: $g = 2$ mm, — ∘ —: $g = 2.5$ mm, other parameters are the same as in Fig. 3.

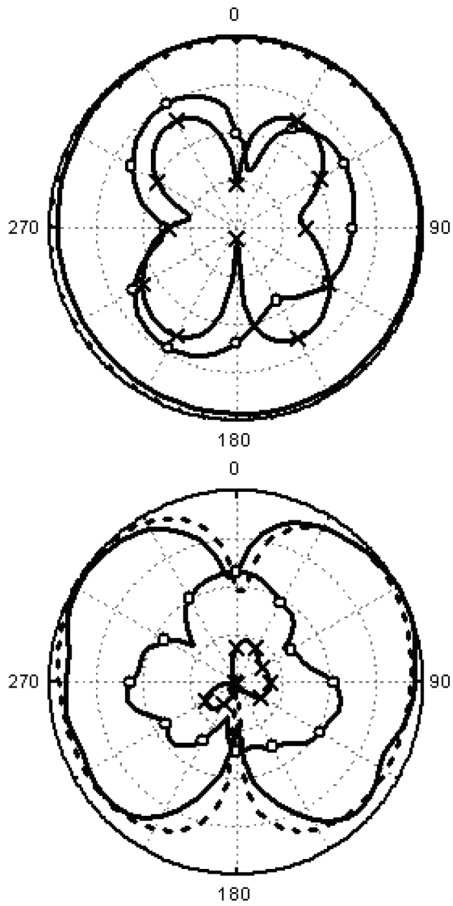


Fig. 8. Radiation pattern at 1.495 GHz: (a) $x - y$ plane, (b) $x - z$ plane, ——: measured $E_\theta$, – – –: simulated $E_\theta$, — ∘ —: measured $E_\phi$, — × —: simulated $E_\phi$, 10 dB per division on radials, all parameters are the same as in Fig. 3.

is nearly omnidirectional. The cross-polarization is about 10 dB lower than the co-polarization. The measured peak gain is 0.7 dBi.

Fig. 9 shows the measured antenna gain which is positive over the whole band. The gain is lower than that of conventional dipoles because part of the currents along the folded lines flow in opposite direction, and their radiated fields partially cancel each other. Fig. 10 shows the measured radiation efficiency of the proposed antenna exceeds 65% over

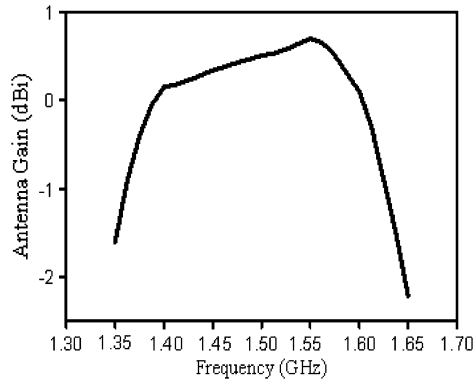


Fig. 9. Measured antenna gain, other parameters are the same as in Fig. 3.

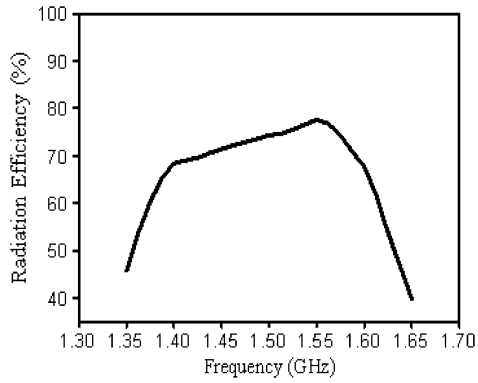


Fig. 10. Measured total radiation efficiency, including impedance mismatch effect, other parameters are the same as in Fig. 3.

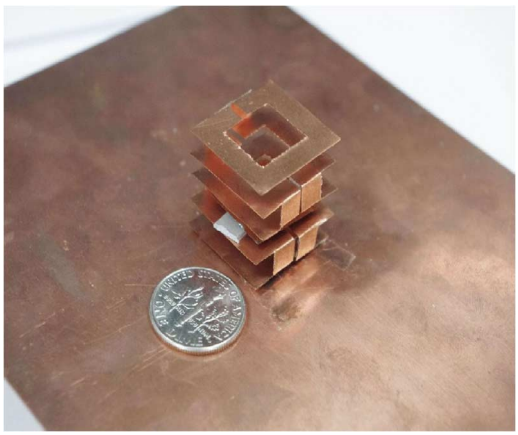

Fig. 11. Photograph of the proposed antenna beside a dime.

the whole band, which is obtained using the full 3-D pattern integration in the anechoic chamber of our laboratory.

Fig. 11 shows the photograph of the proposed antenna. Four paper pads are inserted to make the structure rigid. A slight frequency shift may be contributed by these paper pads.

## IV. Effect of Ground Plane Size

The effect of ground plane size on the antenna performance has been analyzed. The bandwidth of the antenna with a larger ground plane, for example, 400 mm × 400 mm or $2\lambda \times 2\lambda$, is about 13.8%, and the peak gain appears at $\theta = 45^\circ$. The bandwidth of the antenna with a smaller

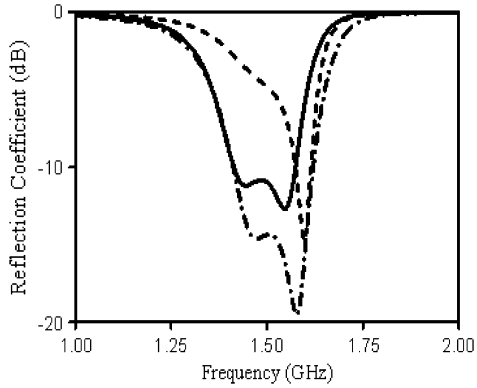


Fig. 12. Simulated reflection coefficients with different ground plane sizes, ——: $G_x = 130$, $G_y = 110$ mm, – – –: $G_x = 50$, $G_y = 50$ mm, – · –: $G_x = 400$, $G_y = 400$ mm, other parameters are the same as in Fig. 3 except the ground plane size.

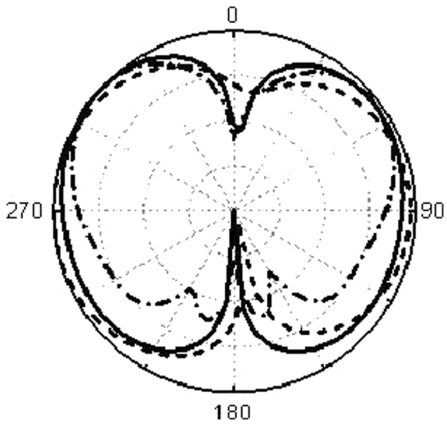


Fig. 13. Simulated $E_\theta$ in the $x-z$ plane at 1.6 GHz with different ground plane sizes, ——: $G_x = 130, G_y = 110$ mm, – – –: $G_x = 50, G_y = 50$ mm, – · –: $G_x = 400, G_y = 400$ mm, 10 dB per division on radials, all parameters are the same as in Fig. 3.

ground plane, for example, 50 mm × 50 mm or $0.25\lambda \times 0.25\lambda$, is about 2.5%, and the peak gain appears at $\theta = 90^\circ$.

With a smaller ground plane, it is difficult to tune the input impedances of the two resonant modes to 50 Ω at the same time although the impedance bandwidth with a larger ground plane is much wider than that with a smaller one, the radiation pattern is not dipole-like and the gain turns negative in the $x - y$ plane.

An electrically small meander-line antenna of dimension $0.08\lambda$ over a finite ground plane of $0.71\lambda \times 0.71\lambda$ is proposed in [19], the peak gain appears at $\theta = 45^\circ$. A dual-meander-line antenna of dimension $0.12\lambda$ placed at the center of a $0.73\lambda \times 0.73\lambda$ ground plane is proposed in [20]. It seems that by nomenclature, a small antenna is referred to the radiator itself, not concerning the size of the ground plane.

In summary, the ground plane does affect the radiation pattern significantly. The proposed antenna can be used for FM broadcasting if the operating frequency is scaled down to 88–108 MHz. For FM broadcasting, the ground plane is usually implemented beneath the soil surface, hence only the structure above the ground is of more concern. This antenna can also be installed in a wireless device with a vertical ground plane. The bandwidth in terms of VSWR remains wide over which the radiation pattern remains dipole-like.

In this design, the ground plane does affect the radiation pattern and the input impedance. The ground plane size over the range from

$0.55\lambda \times 0.65\lambda$ to $0.65\lambda \times 0.75\lambda$ meets the three design goals: (1) The radiation pattern is dipole-like with positive gain in the $x-y$ plane, (2) the antenna structure above the ground plane is smaller than one-tenth of a wavelength, and (3) the $-10$ dB impedance bandwidth is more than 10%. If the ground plane is smaller than $0.55\lambda \times 0.65\lambda$, the impedance matching becomes poor and the impedance bandwidth is reduced. If the ground plane is larger than $0.65\lambda \times 0.75\lambda$, the main beam is steered toward $\theta = 45^\circ$, violating the first design goal.

In this work, the ground plane size of $0.55\lambda \times 0.65\lambda$ gives a broad band in reflection coefficient and a dipole-like radiation pattern.

## V. Conclusions

A small antenna with broad bandwidth has been designed and measured. Its dimension is about $0.1\lambda \times 0.1\lambda \times 0.098\lambda$ and is mounted on a horizontal ground plane size of $0.55\lambda \times 0.65\lambda$ at the center frequency of 1.495 GHz, its fractional bandwidth is 10.8% with VSWR of less than 2, its radiation pattern in the $x-y$ plane is nearly omnidirectional. The ground plane size is optimized to meet the three design goals: Dipole-like radiation pattern with positive gain in the $x-y$ plane, smaller than $\lambda/10$ of structure size above ground, and more than 10% of impedance bandwidth. The measured radiation efficiency exceeds 65% over the whole band. The broadband performance is achieved by proximity coupling between the dual-meander folded loop and the disk-loaded monopole.

## References


[1] J. S. McLean, "A re-examination of the fundamental limits on the radiation Q of electrically small antenna," *IEEE Trans. Antennas Propag.*, vol. 44, no. 5, pp. 672–676, May 1996.

[2] H. D. Foltz, J. S. Mclean, and G. Crook, "Disk-loaded monopoles with parallel strip elements," *IEEE Trans. Antennas Propag.*, vol. 46, no. 12, pp. 1894–1896, Dec. 1998.

[3] W. Dou and W. Y. M. Chia, "Compact monopole antenna for GSM/DCS operation of mobile handsets," *Electron. Lett.*, vol. 39, no. 22, Oct. 30, 2003.

[4] I. F. Chen and C. M. Chiang, "Multi-folded tapered monopole antenna for wideband mobile handset applications," *Electron. Lett.*, vol. 40, no. 10, May 13, 2004.

[5] N. Behdad and K. Sarabandi, "Bandwith enhancement and further size reduction of a class of miniaturized slot antennas," *IEEE Trans. Antennas Propag.*, vol. 22, no. 8, pp. 1928–1935, Aug. 2004.

[6] R. Azadegan and K. Sarabandi, "A novel approach for miniaturization of slot antenna," *IEEE Trans. Antennas Propag.*, vol. 51, no. 3, pp. 421–429, Mar. 2003.

[7] J. Anguera, C. Puente, E. Martinez, and E. Rozan, "The fractal Hilbert monopole: A two-dimensional wire," *Microwave Opt. Technol. Lett.*, vol. 36, no. 2, pp. 102–104, Jan. 2003.

[8] J. P. Gianvittorio and Y. Rahmat-Samii, "Fractal antennas: A novel antenna miniaturization technique, and applications," *IEEE Antennas Propag. Mag.*, vol. 44, no. 1, pp. 20–36, 2002.

[9] J. Anguera, C. Puente, C. Borja, and J. Soler, "Fractal-shaped antennas: A review," *Wiley Encycl. RF Microwave Eng.*, vol. 2, pp. 1620–1635, 2005.

[10] W. Dou and W. Y. M. Chia, "Small broadband stacked planar monopole," *Microw. Opt. Technol. Lett.*, vol. 27, no. 4, pp. 288–289, Nov. 2000.

[11] T.-H. Chang and J.-F. Kiang, "Broadband dielectric resonator antenna with metal coating," *IEEE Trans. Antennas Propag.*, vol. 55, no. 5, pp. 1254–1259, May 2007.

[12] J. W. Jung, H. J. Lee, and Y. S. Lim, "Broadband flexible meander line antenna with vertical lines," *Microw. Opt. Technol. Lett.*, vol. 49, no. 8, pp. 1984–1987, Aug. 2007.

[13] M. Ali, S. S. Stuchly, and K. Caputa, "A wideband dual meander sleeve antenna," *J. Electromagn. Waves Appl.*, vol. 10, no. 9, pp. 1223–1236, 1996.

[14] H. D. Chen, "Compact broadband microstrip-line-fed sleeve monopole antenna for DTV application and ground plane effect," *IEEE Antennas Wireless Propag. Lett.*, vol. 7, pp. 497–500, 2008.

[15] M. Ali, G. J. Hayes, H. S. Hwang, and R. A. Sadler, "Design of a multiband internal antenna for third generation mobile phone handsets," *IEEE Trans. Antennas Propag.*, vol. 51, no. 7, pp. 1452–1461, July 2003.

[16] C. M. Kruesi, R. J. Vyas, and M. M. Tentzeris, "Design and development of a novel 3-D cubic antenna for wireless sensor networks (WSNs) and RFID applications," *IEEE Trans. Antennas Propag.*, vol. 57, no. 10, pp. 3293–3299, Oct. 2009.

[17] F. Qureshi, M. A. Antoniades, and G. V. Eleftheriades, "A compact and low-profile metamaterial ring antenna with vertical polarization," *IEEE Antennas Wireless Propag. Lett.*, vol. 4, pp. 333–336, 2005.

[18] S. Risco, J. Anguera, A. Andujar, A. Perez, and C. Puente, "Coupled monopole antenna design for multiband handset devices," *Microw. Opt. Technol. Lett.*, vol. 52, no. 2, pp. 359–364, Feb. 2010.

[19] A. Erentok and R. W. Ziolkowski, "Metamaterial-inspired efficient electrically small antennas," *IEEE Trans. Antennas Propag.*, vol. 56, no. 3, pp. 691–707, Mar. 2008.

[20] K. Noguchi, M. Mizusawa, T. Yamaguchi, Y. Okumura, and S. Betsudan, "Increasing the bandwidth of a small meander-line antenna consisting of two strips," *Electron. Commun. Jpn, Part. 2*, vol. 83, no. 10, pp. 35–43, 2000.


# A Dual Band Microstrip-Fed Slot Antenna

Mahmoud N. Mahmoud and Reyhan Baktur

***Abstract*—A simple new design method to achieve a dual band microstrip-fed slot antenna is presented. It is shown that when two slot antennas are placed in series, the spacing between the two antennas can be adjusted to achieve an effective secondary resonance. The new resonance is found to be due to the mutual coupling between the two slot antennas. An approximate circuit model for the dual band antenna is presented to explain the dual band mechanism and to provide a design guideline. The model is validated with a prototype antenna that operates at 4.22 GHz and 5.26 GHz, which are commonly used as the downlink and uplink in satellite communications. Measured results show good return loss at both frequencies, and radiation patterns agree well with the simulations. The proposed antenna has a simple geometry can be easily produced using printed circuit board techniques for applications where compactness and multiband operation are of interest.**

***Index Terms*—Microstrip, multifrequency antennas, mutual coupling, slot antennas.**

## I. Introduction

Slot antennas have appealing features such as low profile, low cost, and ease of integration on planar or non-planar surfaces [1]. An example application is integrating slot antennas with solar panels of small satellites to save surface real estate [1], [3]. While slot antennas are valuable for space applications and self-powered ground sensors [4], most designs are limited to single frequency operation. This communication presents a very simple design where one can achieve a dual band antenna by utilizing coupling between two adjacent slots.

Manuscript received May 11, 2010; revised August 23, 2010; accepted October 07, 2010. Date of publication March 07, 2011; date of current version May 04, 2011

The authors are with the Electrical and Computer Engineering Department, Utah State University, Logan, UT 84341 USA (e-mail: reyhan.baktur@usu.edu).

Color versions of one or more of the figures in this communication are available online at http://ieeexplore.ieee.org.

Digital Object Identifier 10.1109/TAP.2011.2123065